Comparison of Statistical Shape Models Built on Correspondence Probabilities and One-to-One Correspondences

Heike Hufnagel[a,b], Xavier Pennec[a],Jan Ehrhardt[b], Nicholas Ayache[a] and Heinz Handels[b]

[a]INRIA Sopha Antipolis, Asclepios Project, France

[b]Medical Informatics, University Medical Center Hamburg-Eppendorf, Germany

ABSTRACT

In this paper, we present a method to compute a statistical shape model based on shapes which are represented by unstructured point sets with arbitrary point numbers. A fundamental problem when computing statistical shape models is the determination of correspondences between the observations of the associated data set. Often, homologies between points that represent the surfaces are assumed. When working merely with point clouds, this might lead to imprecise mean shape and variability results. To overcome this problem, we propose an approach where exact correspondences are replaced by evolving correspondence probabilities. These are the basis for a novel algorithm that computes a generative statistical shape model. We developed a unified Maximum A Posteriori (MAP) framework to compute the model parameters ('mean shape' and 'modes of variation') and the nuisance parameters which leads to an optimal adaption of the model to the set of observations. The registration of the model on the observations is solved using the Expectation Maximization - Iterative Closest Point algorithm which is based on probabilistic correspondences and proved to be robust and fast. The alternated optimization of the MAP explanation with respect to the observation and the generative model parameters leads to very efficient and closed-form solutions for nearly all parameters. A comparison with a statistical shape model which is built using the Iterative Closest Point (ICP) registration algorithm and a Principal Component Analysis (PCA) shows that our approach leads to better SSM quality measures.

Keywords: statistical shape model, correspondence problem, em-icp, registration, MAP

1. INTRODUCTION

One of the central difficulties of analyzing different organ shapes in a statistical manner is the identification of correspondences between the points of the shapes. As the manual identification of landmarks is not a feasible option in 3D, several preprocessing techniques were developed to automatically find exact one-to-one correspondences between surfaces which are represented by meshes.[1–4] A popular method is to optimize for correspondences and registration transformation as does the Iterative Closest Points (ICP) algorithm[5] for point clouds. More elaborate methods directly combine the search of correspondences and of the statistical shape model (SSM) for a given training set.[6,7] The Minimum Description Length (MDL) approach to statistical shape modeling[8,9] is such a method and has shown to come to good results. For computing a SSM using unstructured point sets, however, the MDL approach is not well- suited because it needs an explicit surface information. Another interesting approach proposes an entropy based criterion to find shape correspondences, but requires implicit surface representations.[10] Other works combine the search for correspondences with shape based classification[11,12] or with shape analysis,[13] however, these methods are not easily adaptable to multiple observations of unstructured point sets. An interesting approach for unstructured point sets focuses only on the mean shape.[14] In all cases, enforcing exact correspondences for surfaces represented by unstructured point sets leads to variability modes that not only represent the organ shape variations but also artificial variations whose importance is linked to the local sampling of the surface points. We argue that when segmenting anatomical structures in image data with important noise, the extracted surface points only represent probable surface locations. Therefore we believe that a method for shape analysis should better rely only on the point locations and not on surface information.

E-mail: h.hufnagel@uke.uni-hamburg.de

In this paper, we address the problem of building a SSM for shape observations represented by unstructured point sets with differing point numbers. In order to replace the assumption of exact correspondences, we pursue a probabilistic concept by aligning the observations in a group-wise registration with the Expectation Maximization - Iterative Closest Point (EM-ICP) algorithm which proved to be robust, precise, and fast.[15] The SoftAssign algorithm[16] has a probabilistic formulation which is closely related but differs in that it gives the same role to the source and the registration target.
In our algorithm, we unify all steps for the SSM construction (computation of the registration transformations, the correspondence probabilities, the mean shape and the modes of variation) in a unique global criterion. This is realized by a Maximum a Posteriori (MAP) estimation of the model and observation parameters. We compute the SSM parameters which best fit the given data set by optimizing the global criterion iteratively with respect to all model and observation parameters. A key part of our method is that we can find a closed-form solution for almost each of the parameters. In particular, the approach solves for the mean shape and the eigenmodes *without* the need of one-to-one correspondences as is usually required by the PCA.
This article focuses on the validation of the work presented in 2007[17] where we showed that our SSM is robust and leads to plausible results for synthetic data as well as brain structures. A comparison of our SSM and a SSM based on exact correspondences in terms of the established measures "generalization ability" and "specificity" is performed for evaluation.
The remainder of this paper is organized as follows: The main steps of our algorithm - the computation of all model parameters (as well as all nuisance parameters) in a unified criterion - is described in section 2. In section 3, the experimental evaluation of the SSM is presented. Section 4 concludes the paper.

2. CONSTRUCTION OF THE STATISTICAL SHAPE MODEL

2.1. Model and Observation Parameters

In the process of computing the SSM, we distinguish strictly between ***model parameters*** and ***observation parameters***. The generative SSM is explicitly defined by 4 ***model parameters***:

- mean shape $\bar{M} \in \mathbb{R}^{3N_m}$ parameterized by N_m points $m_j \in \mathbb{R}^3$,
- eigenmodes v_p consisting of N_m 3D vectors v_{pj},
- associated standard deviations λ_p which describe - similar to the classical eigenvalues in the PCA - the impact of the eigenmodes,
- number n of eigenmodes.

Using the generative model $\Theta = \{\bar{M}, v_p, \lambda_p, n\}$ of a given structure, the shape variations of that structure can be generated by $M_k = \bar{M} + \sum_{p=1}^{n} \omega_{kp} v_p$ with $\omega_{kp} \in \mathbb{R}$ being the deformation coefficients. The shape variations along the modes follow a Gaussian probability with variance λ_p:

$$p(M_k|\Theta) = p(\Omega_k|\Theta) = \prod_{p=1}^{n} p(\omega_{kp}|\Theta) = \frac{1}{(2\pi)^{n/2} \prod_{p=1}^{n} \lambda_p} \exp\left(-\sum_{p=1}^{n} \frac{\omega_{kp}^2}{2\lambda_p^2}\right). \quad (1)$$

with $\Omega_k \in \mathbb{R}^n$ being a vector consisting of the deformation coefficients ω_{kp} associated with shape variation M_k. In order to account for the unknown position and orientation of the model in space, we introduce the random (uniform) rigid or affine transformation T_k. A model point m_j can then be deformed and placed by $T_k \star m_{kj} = T_k * (\bar{m}_j + \sum_p \omega_{kp} v_p)$. Finally, we specify the sampling of the model surface: Each sampling (e.g. observation) point s_{ki} is modeled as a Gaussian measurement of a (transformed) model point m_{kj}. The probability of the observation $p(s_{ki}|m_{kj}, T_k)$ knowing the originating model point m_{kj} is given by
$p(s_{ki}|m_{kj}, T_k) = (2\pi)^{-3/2}\sigma^{-1} \exp(-\frac{1}{2\sigma^2}(s_{ki} - T_k \star m_{kj})^T.(s_{ki} - T_k \star m_{kj})$. As we do not know the originating model point for each s_{ki}, the probability of a given observation point s_{ki} is described by a Mixture of Gaussians and the probability for the whole scene S_k becomes:

$$p(S_k|M, T_k) = \prod_{i=1}^{N_k} \frac{1}{N_m} \sum_{j=1}^{N_m} p(s_{ki}|m_{kj}, T_k). \quad (2)$$

We summarize the ***observation parameters*** as $Q_k = \{\Omega_k, T_k\}$. Notice that the correspondences are hidden parameters that do not belong to the observation parameters of interest.

2.2. Derivation of the Global Criterion Using a MAP Approach

When building the SSM, we deal with the inverse problem of the approach in section 2.1: We have N observations $S_k \in \mathbb{R}^{3N_k}$, and we are interested in the parameters linked to the observations $Q = \{Q_k\}$ as well as the unknown model parameters Θ. In order to determine all parameters of interest, we optimize a MAP estimation on Q and Θ rather than an Maximum Likelihood (ML) estimation to take into account that Q and Θ are not independent.

$$\text{MAP} \quad = \quad -\sum_{k=1}^{N} \log(p(Q_k, \Theta|S_k)) = -\sum_{k=1}^{N} \log\left(\frac{p(S_k|Q_k,\Theta)p(Q_k|\Theta)p(\Theta)}{p(S_k)}\right). \tag{3}$$

As $p(S_k)$ does not depend on Θ and $p(\Theta)$ is assumed to be uniform, the global criterion integrating our unified framework is the following:

$$C(Q,\Theta) = -\sum_{k=1}^{N} \left(\log(p(S_k|Q_k,\Theta)) + \log(p(Q_k|\Theta))\right). \tag{4}$$

The first term describes the ML criterion (2) whereas the second term is the prior on the deformation coefficients ω_{kp} as described in (1). Dropping the constants, our criterion simplifies to $C(Q,\Theta) \sim \sum_{k=1}^{N} C_k(Q_k,\Theta)$ with

$$C_k(Q_k,\Theta) = \sum_{p=1}^{n}\left(\log(\lambda_p) + \frac{\omega_{kp}^2}{2\lambda_p^2}\right) - \sum_{i=1}^{N_k}\log\left(\sum_{j=1}^{N_m}\exp\left(-\frac{\|s_{ki} - T_k \star m_{kj}\|^2}{2\sigma^2}\right)\right). \tag{5}$$

This equation is the heart of the unified framework for the model computation and its fitting to observations. By optimizing it alternately with respect to the operands in $\{Q,\Theta\}$, we are able to determine all parameters we are interested in. Starting from the initial model parameters Θ, we fit the model to each of the observations (section 2.3). Next, we fix the observation parameters Q_k and update the model parameters (section 2.4). Some terms will recur in the different optimizations, so we introduce the following notation for the derivation of the second term $\xi_{kij}(T_k, \Omega_k, \bar{M}, v_p, \lambda_p) = \log\sum_{j=1}^{N_m}\exp\left(\frac{-\|s_{ki}-T_k\star m_{kj}\|^2}{2\sigma^2}\right)$ with respect to one of the function's parameters (let's say x):

$$\frac{\partial\xi}{\partial x} = \sum_{j=1}^{N_m}\gamma_{kij}\frac{(s_{ki} - T_k\star m_{kj})^T}{\sigma^2}\quad\frac{\partial(s_{ki} - T_k\star m_{kj})}{\partial x} \tag{6}$$

where the weights $\gamma_{ijk} = \exp\left(-\frac{\|s_{ki}-T_k\star m_{kj}\|^2}{2\sigma^2}\right)\left[\sum_{l=1}^{N_m}\exp\left(-\frac{\|s_{ki}-T_k\star m_{kl}\|^2}{2\sigma^2}\right)\right]^{-1}$ are sometimes interpreted as soft labels/correspondences.

2.3. Mapping the Model to the Observations

2.3.1. Optimization with respect to the Transformations

The registration transformation is computed with an affine EM-ICP algorithm. In the following, we summarize the mathematical steps, for more details please refer to the work of Granger et al. about the rigid EM-ICP.[15]
As no closed form solution exists for the optimization of criterion (2), we employ an EM algorithm where the correspondence probabilities between S_k and M are modeled as the hidden variable $H_k \in \mathbb{R}^{N_k\times N_m}$. An instance point s_{ki} corresponds to a model point m_j with probability $E(H_{k_{ij}})$. By computing the expectation of the log-likelihood of the complete data distribution with T_k fixed, we find in the *expectation step* $E(H_{k_{ij}}) = \gamma_{kij}$. As defined above, the γ_{kij} represent the weights of each pair (s_{ki}, m_j) in the criterion. Next, $T_k = \{A_k, t_k\}$ is computed in the *maximization step* by maximizing the global criterion in (5) with all γ_{kij} fixed in a closed-form solution. Here, $A_k \in \mathbb{R}^{3\times3}$ is the affine transformation matrix and $t_k \in \mathbb{R}^3$ the translation vector. The implementation of the EM-ICP algorithm is realized in a multi-scaling frame regarding the variance. The EM-ICP is initialized with a great variance to ensure that shape positions, rotation and sizes are aligned. The variance is then reduced in each iteration to cover for shape details. $\sigma_{initial}$ and its decrease rate have to be carefully adapted to the data at hand (σ_{final} should be in the order of the average point distance).

2.3.2. Optimization with respect to the Deformation Coefficients

The observation parameter T_k and Θ are fixed, and we compute the ω_{kp} which solve $\partial C_k(Q_k, \Theta)/\partial \omega_{kp} = 0$. This leads to a matrix equation of the form

$$\Omega_k = (B_k - \sigma^2 \Lambda_{nn})^{-1} \vec{d}_k \tag{7}$$

with

$$d_{kp} = \sum_{i=1}^{N_k} \sum_{j=1}^{N_m} \gamma_{kij} (s_{ki} - t_k - A_k \bar{m}_j)^T A_k v_{pj}, \quad d_{kp} \in \mathbb{R}$$

and

$$b_{kqp} = \sum_{i=1}^{N_k} \sum_{j=1}^{N_m} \gamma_{kij} v_{qj}^T A_k^T A_k v_{pj}, b_{kqp} \in \mathbb{R}, \quad b_{kqp} = b_{kpq}.$$

Hence, in order to compute the ω_{kp}, for each k the matrix B_k and the vector $\vec{d}_k$ have to be evaluated.

2.4. Learning the Model from the Observations

2.4.1. Optimization with respect to the Standard Deviations

The computation of the optimal standard deviation λ_p with parameters $\bar{M}, v_p$ and Q_k fixed is simply:

$$\frac{\partial C(Q, \Theta)}{\partial \lambda_p} = \sum_{k=1}^{N} \left(\frac{1}{\lambda_p} - \frac{\omega_{kp}^2}{\lambda_p^3} \right) = 0 \quad \Leftrightarrow \quad \lambda_p^2 = \frac{1}{N} \sum_{k=1}^{N} \omega_{kp}^2. \tag{8}$$

2.4.2. Optimization with respect to the Mean Shape

Setting $\partial C(Q, \Theta)/\partial \bar{m}_j$ to 0 and using the general derivation presented in (6), we find

$$\bar{m}_j = \left(\sum_{k=1}^{N} \sum_{i=1}^{N_k} \gamma_{kij} A_k^T A_k \right)^{-1} \sum_{k=1}^{N} \sum_{i=1}^{N_k} \gamma_{kij} A_k^T (s_{ki} - t_k - A_k \sum_{p=1}^{n} \omega_{kp} v_{pj}) \tag{9}$$

2.4.3. Optimization with respect to the Eigenmodes

The parameters $\lambda_p, \bar{M}$ and Q_k are fixed. Let us first define the matrix $V \in \mathbb{R}^{3N_m \times n}$ containing the eigenmodes $\vec{v}_p \in \mathbb{R}^{3N_m}$ in its columns. The $\vec{v}_{pj} \in \mathbb{R}^3$ referred to in the equations are the eigenmode information associated to point $\bar{m}_j$. As we want the eigenmodes to be orthonormal, we add a Lagrange multiplier by introducing the symmetric matrix $Z \in \mathbb{R}^{n \times n}$ to our global criterion in the form: $\Lambda = C + \frac{1}{2} tr\left(Z(V^T V - I_{n \times n})\right)$. Deriving the Lagrangian with respect to $\vec{v}_{pj}$ gives in the rigid case

$$\frac{\partial \Lambda}{\partial \vec{v}_{pj}} = \sum_{q=1}^{n} z_{qp} \vec{v}_{qj} - \sum_{q=1}^{n} b_{pq} \vec{v}_{qj} + q_{pj}$$

where

$$\vec{q}_{pj} = \frac{1}{\sigma^2} \sum_{k=1}^{N} \sum_{i=1}^{N_k} \gamma_{kij} (s_{ki} - t_k - A_k \bar{m}_j)^T \, \omega_{kp} A_k, \quad q_{pj} \in \mathbb{R}^3$$

and

$$b_{pqj} = \frac{1}{\sigma^2} \sum_{k=1}^{N} \sum_{i=1}^{N_k} \gamma_{kij} \omega_{kq} \omega_{kp} I_{3\times 3} \quad b_{pqj} \in \mathbb{R}^{3\times 3}.$$

Hence we find $\sum_{q=1}^{n} \vec{v}_{jq}(z_{qp} + b_{pqj}) = \vec{q}_{jp}$. We approach the problem regarding each of the N_m bands $[V]_{\{j\}} \in \mathbb{R}^{3\times n}$ of matrix $V \in \mathbb{R}^{3N_m \times n}$ separately with $[V]_{\{j\}} = [\vec{v}_{j1}, ..., \vec{v}_{jq}, ..., \vec{v}_{jn}]$ and $[V]_{\{j\}} (B_j + Z) = [Q]_{\{j\}}$. We iterate the following two steps until $\|V^{t+1} - V^t\|^2 \leq \epsilon$.

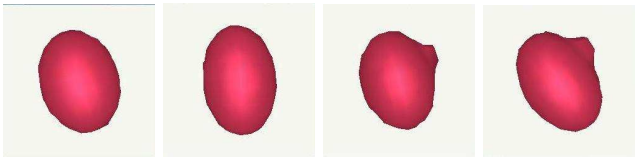

Figure 1. Observation examples of a synthetic training data set featuring two distinctive shape classes (ellipsoids with bump and ellipsoids without bumps).

1. For Z known, we compute V: $[V]_{\{j\}} = [Q]_{\{j\}} (B_j + Z)^{-1}$ for all model point indices j. To enforce V to be orthonormal, we apply first a singular value decomposition $V = USR^T$ and then replace V by UR^T.
2. For all $[V]_{\{j\}}$ known, we determine Z: $Z = V^T \tilde{Q}$ with $[\tilde{Q}]_{\{j\}} = [Q]_{\{j\}} - [V]_{\{j\}} B_j$. As Z has to be symmetric, we set $Z \leftarrow \frac{1}{2}(Z + Z^T)$.

3. EXPERIMENTS AND RESULTS

In order to assess the quality of the SSM based on correspondence probabilities, we compared it to a SSM based on exact correspondences built for the same training data set. In a first test, we apply the two SSMs to a synthetic training data set which contains two distinguished shape classes (section 3.1). In a second test, we apply the two SSMs to brain data and quantify the results by evaluating the two performance measures 'generalization ability' and 'specificity' (section 3.1.1).
The SSM based on exact correspondences is generated in a similar manner as proposed in[4]:

1. Group-wise registration using the ICP algorithm.
2. Computing the mean shape on the exact correspondences found by the ICP.
3. Applying a PCA to determine the eigenmodes.

In the following, it will be called SSM-ICP.

3.1. Correspondence Probabilities versus Exact Correspondences: A Case Study

We argue that the determination of correspondences between unstructured point sets is especially difficult when one shape features a certain structure detail and the other one does not. For an experimental evaluation, we generated a training data set containing two distinctive shape classes. The data set consisted of 9 ellipsoids featuring a bump and 9 ellipsoids without bump. We deformed them with different affine transformations in order to obtain varying ellipsoid shapes. For 4 observation examples, see figure 1.
We computed our SSM as well as the SSM-ICP for the ellipsoid data and compared the results. As initial mean shape, we chose an observation of the class without bump. The respective resulting mean shapes and deformations according to the first mode of variation can be seen in figure 2.

Results: The SSM based on the EM-ICP models the whole data set, it is able to represent the ellipsoids featuring a bump and those without as that deformation information is included in its variability model.
The SSM based on the ICP is not able to model the bump. This is due to the fact that the ICP only takes into account the closest point when searching for correspondence, thus, the point on top of the bump is not involved in the registration process. The EM-ICP, however, analyzes the correspondence probability of *all* points, therefore, also the point on top of the bump is matched. We illustrated these two concepts in figure 3.

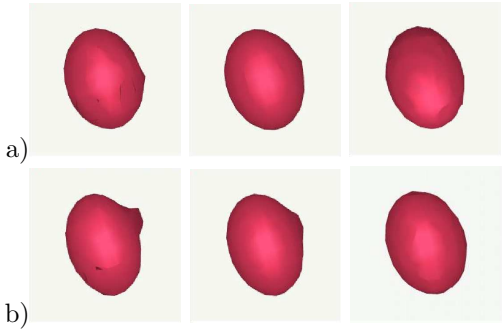

Figure 2. Results of a SSM built on exact correspondences (a) and of a SSM built on correspondence probabilities (b) for the training data shown in figure 1. Mean shape (middle), and the mean shape deformed with respect to the first eigenmode, left:$\bar{M} - 3\lambda_1\vec{v}_1$ and right:$\bar{M} + 3\lambda_1\vec{v}_1$.

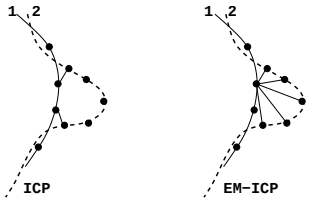

Figure 3. *One-to-one correspondence versus correspondence probabilities. Left: ICP registration, each point on contour 1 corresponds to the closest point on contour 2. Right: EM-ICP registration, each point on contour 1 corresponds with a certain probability to all points on contour 2.*

3.1.1. Generalization Ability and Specificity for a Brain Structure Data Set

In order to assess the quality of the generative SSM, we analyse the two established measures *generalization ability* and *specificity* as proposed in[18] for our SSM and the SSM-ICP. A good generalization ability is important for recognition purposes as a SSM must be able to adopt the shape of a new - unseen - observation which comes from the same (anatomical) structure type. The specificity of a SSM must be high for shape prediction purposes as the SSM should only adopt shapes similar to the ones in the underlying training set.
The training data set for this experiment consists of $N = 24$ left segmented putamens (approximately $20mm \times 20mm \times 40mm$) which are represented by min 994 and max 1673 points, see Figure 4a) and b) for some shape examples. The MR images contain $255 \times 255 \times 105$ voxels of size $0.94mm \times 0.94mm \times 1.50mm$. The data was collected in the framework of a study on hand dystonia.
We generated the SSM with the following parameters: Number of eigenmodes $n = 18$, initial sigma in the EM-ICP $\sigma = 4mm$, variance multi-scaling factor of the EM-ICP 0.85, and 10 EM-ICP iterations which results in a final $\sigma_{final} = 0.92mm$. Figure 4 shows the resulting mean shape and the deformations of the left putamen according to the variation modes.
We generated a SSM-ICP for the same data set with again 18 eigenmodes.

The generalization ability is tested in a series of leave-one-out experiments. We analyse how closely the SSM matches an unknown observation. The SSM is first aligned with the new observation. Then, equation (7) is evaluated to find the deformation coefficients ω_{kp}. The resulting coefficients are used to deform the aligned SSM in order to optimize the matching. Finally, the distance of the deformed SSM to the left-out observation is measured.
We performed this test for 7 different unknown observations and different numbers of eigenmodes. The results obtained by our SSM and the SSM-ICP are shown in table 1.

In order to test the **specificity**, we generated random shapes x which are uniformly distributed with σ equal to the standard deviation of the SSM. We then computed the average and maximal distances of the random shapes to the closest observation in the training data set. The results for both SSMs and 500 random shapes can be

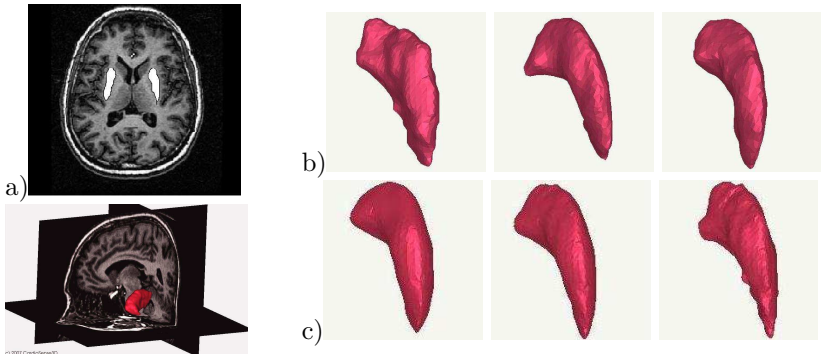

Figure 4. *Shape analysis of the putamen. a) CT-images with segmented left putamen. b) Observation examples of the data set. c) Mean shape (middle) and its deformations according to the first eigenmode ($\bar{M} - 3\lambda_1\vec{v}_1$ and $\bar{M} + 3\lambda_1\vec{v}_1$).*

Table 1. *Shape distances found in generalization experiments (7 leave-one-out tests) with our SSM approach and with the SSM-ICP approach.*

	SSM-ICP	our SSM
5 variation modes		
average mean distance + standard deviation in mm	0.634 ± 0.090	0.466 ± 0.104
average maximal distance + standard deviation in mm	4.478 ± 0.927	2.578 ± 0.729
10 variation modes		
average mean distance + standard deviation in mm	0.623 ± 0.099	0.453 ± 0.102
average maximal distance + standard deviation in mm	4.449 ± 0.909	2.465 ± 0.690
18 variation modes		
average mean distance + standard deviation in mm	0.610 ± 0.089	0.447 ± 0.101
average maximal distance + standard deviation in mm	4.388 ± 0.930	2.426 ± 0.712

Table 2. *Shape distances found in specificity experiments (500 random shapes) with our SSM approach and with an ICP+PCA approach using 18 eigenmodes.*

	SSM-ICP	our SSM
average mean distance + standard deviation in mm	0.515 ± 0.117	0.452 ± 0.020

seen in table 2.
Results: For both performance measures, our SSM achieved superior results compared to the SSM-ICP. Especially the values of the maximal distance show the benefit of the new approach.
In the leave-one-out experiment, we showed that the number of eigenmodes is controlling the accuracy of the deformed SSM. The distance decreases when more variation modes are used. Also, the percental distance decrease between the results with 5 variation modes and the results with 18 eigenmodes is slightly less with the SSM-ICP (about 5% with our SSM and 3% with the SSM-ICP). These results suggest that our SSM is better able to cover for shape details.

4. DISCUSSION

We proposed a novel algorithm to generate a statistical shape model for unstructured point sets. The computation of the SSM is based on correspondence probabilities instead of exact correspondences. The approach does not need any surface information, it can be used for non-spherical shapes and can be adapted to applications on data sets with different topologies as the connectivity between points does not play a role. We developed a mathematically sound and unified framework for the computation of model parameters and observation parameters and succeeded in determining a closed form solution for optimizing the associated criterion alternately for all parameters. Experiments showed that our algorithm works well and leads to plausible results for different kind of data. It seems to be stable even for small numbers of observations. In an experimental evaluation, we compared the performance of our SSM to a SSM built on exact correspondences (Iterative Closest Points

and Principal Component Analysis) for the same data sets. On a data set featuring a typical correspondence problem, our approach succeeded to compute a representing mean shape and variability model whereas the SSM based on exact correspondences failed. In an experiment on real data, we showed that our approach leads to a better accuracy for the two established SSM measures 'generalization ability' and 'specificity'.
From a theoretical point of view, a very powerful feature of our method is that we are optimizing a unique criterion. Thus, the convergence is ensured. However, the practical convergence rate has to be investigated more carefully. For instance, a fast decrease of the multi-scale variance σ^2 easily freezes the model in local minima. For further validation, we intend to study other kinds of data (e.g. hippocampus or ganglion) whose shapes are less convex than the putamen. Indeed, this type of data is typically requiring the use of SSMs for their automatic segmentation. In order to ensure robustness, we will extend the distance measure in the EM-ICP to include the normals.

Acknowledgments

The MR images as well as the segmentations of the putamen data were kindly provided by the Hôpital La Pitié-Salpêtrière, Paris, France.
This work is supported by a grant from the DFG, HA2355.

REFERENCES

1. C. Lorenz and N. Krahnstoever, "Generation of point-based 3D statistical shape models for anatomical objects.," *Computer Vision and Image Understanding* **77**, pp. 175–191, 2000.
2. F. L. Bookstein, "Landmark methods for forms without landmarks: morphometrics in group differences in outline shapes.," *Medical Image Analysis* **1**, pp. 225–243, 1996.
3. M. Styner, G. Gerig, J. Lieberman, D. Jones, and D. Weinberger, "Statistical shape analysis of neuroanatomical structures based on medial models," *Medical Image Analysis* **7**, pp. 207–220, 03.
4. F. Vos, P. de Bruin, G. Streeksa, M. Maas, L. van Vliet, and A. Vossepoel, "A statistical shape model without using landmarks," in *Proceedings of the ICPR'04.*, **3**, pp. 714–717, 2004.
5. P. J. Besl and N. D. McKay, "A method for registration of 3D shapes," *IEEE Transactions PAMI* **14**, pp. 239–256, 1992.
6. Z. Zhao and E. K. Theo, "A novel framework for automated 3D PDM construction using deformable models," in *Medical Imaging 2005, SPIE Proc*, **5747**, pp. 303–314, 2005.
7. H. Chui, L. Win, R. Schultz, J. Duncan, and A. Rangarajan, "A unified non-rigid feature registration method for brain mapping.," *Medical Image Analysis* **7**, pp. 113–130, 2003.
8. R. Davies, C. Twining, and T. Cootes, "A minimum description length approach to statistical shape modeling," *IEEE Transactions Medical Imaging* **21(5)**, pp. 525–537, May 2002.
9. T. Heimann, I. Wolf, T. Williams, and H. Meinzer, "3D active shape models using gradient descent optimization of description length," in *Proceedings of the IPMI'05*, **3565**, pp. 566–577, 2005.
10. J. Cates, M. Meyer, P. Fletcher, and R. Whitaker, "Entropy-based particle systems for shape correspondences.," in *Proceedings of the MICCAI'06*, **1**, pp. 90–99, 2006.
11. A. Tsai, W. M. Wells, S. K. Warfield, and A. S. Willsky, "An EM algorithm for shape classification based on level sets," *Medical Image Analysis* **9**, pp. 491–502, 2005.
12. S. Kodipaka, B. Vemuri, A. Rangarajan, C. Leonard, I. Schmallfuss, and S. Eisenschenk, "Kernel fisher discriminant for shape-based classification in epilepsy," *Medical Image Analysis* **11**, pp. 79–90, 2007.
13. A. Peter and A. Rangarajan, "Shape analysis using the Fisher-Rao Riemannian metric: Unifying shape representation and deformation," in *IEEE Transactions ISBI'06*, pp. 1164–1167, 2006.
14. H. Chui, A. Rangarajan, J. Zhang, and C. Leonard, "Unsupervised learning of an atlas from unlabeled point-sets," *IEEE Transactions on PAMI'04* **26**, pp. 160–172, 2004.
15. S. Granger and X. Pennec, "Multi-scale EM-ICP: A fast and robust approach for surface registration.," in *Proceedings of the ECCV'02*, *LNCS* **2525**, pp. 418–432, 2002.
16. A. Rangarajan, H. Chui, and F. L. Bookstein, "The softassign procrustes matching algorithm," in *Proceedings of the IPMI'97*, **1230**, pp. 29–42, 1997.

17. H. Hufnagel, X. Pennec, J. Ehrhardt, H. Handels, and N. Ayache, "Shape analysis using a point-based statistical shape model built on correspondence probabilities," in *Proceedings of the MICCAI'07*, **1**, pp. 959–967, 2007.
18. M. Styner, K. Rajamani, L. Nolte, G. Zsemlye, G. Székely, C. Taylor, and R. Davies, "Evaluation of 3D correspondence methods for model building," in *Proceedings for the IPMI'03*, **2732**, pp. 63–75, 2003.